CHAPTER 3

Results and Discussion

Cotton cloths were pretreated with $SiCl_4$ and followed by surface modification using POTS, DMDCS, and SA. Morphology, chemical composition, cross-linking, crystallization, and wettability of the cotton cloths were characterized. The results obtained from each characterization techniques are as follows:

3.1 Characterization of Morphology and Chemical Composition by Scanning Electron Microscopy (SEM) and Energy Dispersive Spectrometer (EDS)

SEM and EDS were employed to characterize the surface and the element composition before and after treatment. For the treatment cotton cloth, the first layer was deposited by $SiCl_4$ and the second layer was deposited by the high degree of hydrophobic agent. The hydrophobic agents are POTS, DMDCS, and SA.

3.1.1 Untreated Cotton Cloth

Untreated cotton cloth from Warorod market was washed and dried at room temperature for overnight. The morphology of the untreated cotton cloth is displayed in Figure 3.1. The SEM images show the surface of the cotton cloth at 500x and 3,000x of magnifications, the cotton fibers show smooth surface with approximate diameter of 5-10 μm.

ลิขสิทธิ์มหาวิทยาลัยเชียงใหม่
Copyright© by Chiang Mai University
All rights reserved

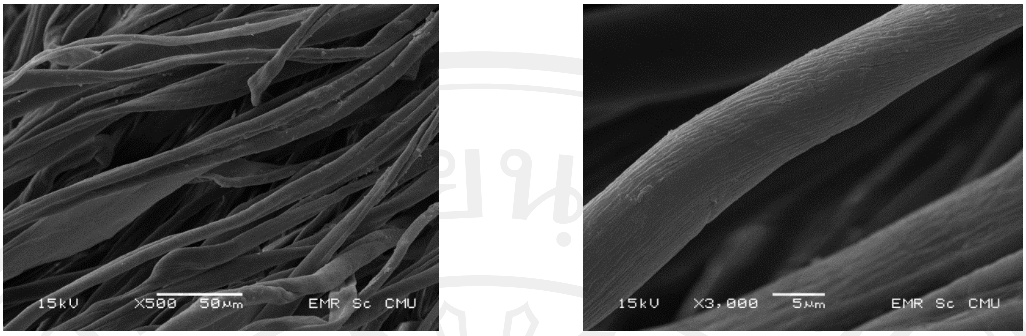

(A) (B)

Figure 3.1 SEM images of untreated cotton cloth at (A) 500x and (B) 3000x magnification.

3.1.2 $SiCl_4$-Treated Cotton Cloth

The objective is to develop a general approach for fabrication of nanoscale inorganic surface layers on cotton cloth. Inorganics are much more easily surface-modified for a range of applications, such as catalysis, adhesion, wettability, biocompatibility, sensing, and protective coating. In order to grow the highest amount of $SiCl_4$ on the surface of the cotton fibers, the parameters such as deposition time, cycle number, and repeating time were optimized.

3.1.2.1 Determination of the Deposition Time for Growing $SiCl_4$

Figure 3.2 shows SEM images illustrating the morphological appearance of untreated cotton cloth and $SiCl_4$ modified cotton cloth at different deposition times.

ลิขสิทธิ์มหาวิทยาลัยเชียงใหม่
Copyright© by Chiang Mai University
All rights reserved

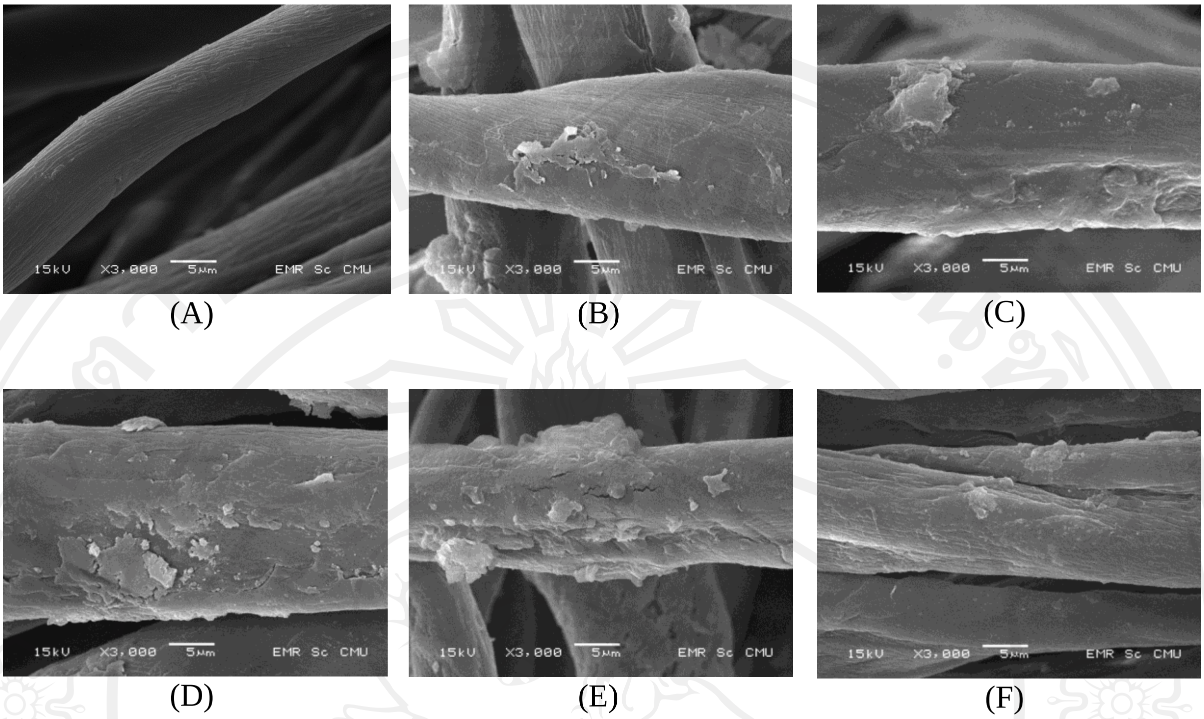

(A) (B) (C)

(D) (E) (F)

Figure 3.2 3000 x magnification SEM images of the $SiCl_4$-treated cotton cloth at various deposition times (A) = 0 min, (B) = 5 min, (C) = 10 min, (D) = 15 min, (E) = 20 min, and (F) = 30 min.

The surface of the $SiCl_4$-cotton cloth at different deposition times from 5 min to 30 min exhibit the more roughness surface due to $SiCl_4$ coating. In magnification view of 3,000x, the agglomeration of the $SiCl_4$ is clearly observed on the cotton cloth surface. It is found that the particle sizes are big with non-uniform structure when deposition time increases indicating the accumulation of $SiCl_4$, while the surface of untreated cotton cloth show the smoother surface. Therefore, it can be confirmed that the surface of cotton is successfully coated by $SiCl_4$. Nanoscale silica layer was prepared via reactions (multiple cycles if necessary) between -OH groups (alcohol or silanol) with $SiCl_4$ followed by hydrolysis (air exposure). These silica layer reacts as inorganics, as assessed by their reactivities toward several silanes. In deposition process, the cotton cloth structure uses hydroxyl groups to bond with Si vapor to form Si-OH that was demonstrated by Quarmyne and Chen [15]. Kango *et al.*

ลิขสิทธิ์มหาวิทยาลัยเชียงใหม่
Copyright© by Chiang Mai University
All rights reserved

studied the surface modification of nanoparticles by chemical treatments (such as the absorption of silane coupling agents), which is a useful method to improve the dispersion stability of nanoparticles in various liquid media. The concept of silane coupling agents, a nanoparticle modified with a 3-methacryloxypropyl trimethoxysilane coupling agent. The surface of the unmodified nanoparticle was covered only with -OH groups, while the surface of the silane-modified nanoparticle was covered with 3-methacryloxypropyl trimethoxysilane molecules. The modified nanoparticles behave differently within organic solvents or polymer matrices compared to unmodified nanoparticles, e.g., the modified nanoparticles show comparatively better dispersion in both media [29].

Furthermore, EDS was employed to investigate the chemical composition of $SiCl_4$ deposited on cotton cloth surface with different deposition times. $SiCl_4$ reacts readily with water. $SiCl_4$ is hydrolysed via the following reaction; $SiCl_4 + 2H_2O \rightarrow SiO_2 + 4HCl$. Therefore, clusters on cotton cloth surface are SiO_2. The cotton cloth is cellulose, which consists of among the C and O components. Si can be observed, the Si peak that appears at 1.739 keV indicating $SiCl_4$ coating, while C and O peaks are observed due to the structure of cellulose of cotton cloth fibers at 0.277 and 2.120 keV, respectively, shown in Figure 3.3 (The EDS spectra of the untreated cotton cloth and the $SiCl_4$-treated cotton cloth at 20 min of deposition time).

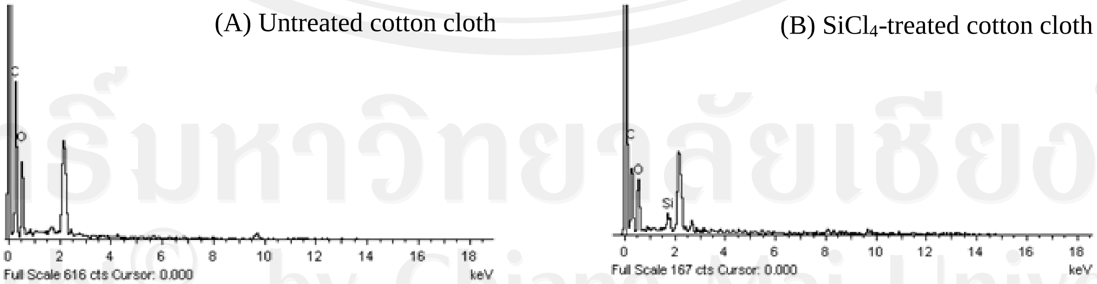
(A) Untreated cotton cloth

(B) $SiCl_4$-treated cotton cloth

Figure 3.3 EDS spectra of (A) untreated cotton cloth and (B) $SiCl_4$-treated cotton cloth.

ลิขสิทธิ์มหาวิทยาลัยเชียงใหม่
Copyright© by Chiang Mai University
All rights reserved

SiO_2 particles are a class of nontoxic, stable, and high thermal resistant inorganic fillers. Owing to these excellent properties, they are used in many fields, such as rubbers, plastics, coatings, printings, and cosmetics. However, the strong hydrophilicity arising from the hydroxyl group (-OH) on the silica surface brings about the nanoparticles to be easily agglomerated and hardly dispersible in polymer matrix. Surface modification of the silica particles with organic modifiers can decrease the amount of hydroxyl groups on the silica surface and change the particles from hydrophilic to hydrophobic entities. Shu Kang *et al.* focused on the emulsion polymerization with emulsifier in the presence of nanoparticles. Since the surface hydroxyl groups of silica particles were hydrophilic, when modified by hydrophobic organic group with long chain could act as an emulsifier to stabilize the particles. Thus, it is also possible to prepare polymer/SiO_2 composite emulsion without an emulsifier, which is confirmed by groups in soap-free emulsion polymerization of methyl methacrylate and hydroxyethyl methacrylate in the presence of colloidal SiO_2 [30].

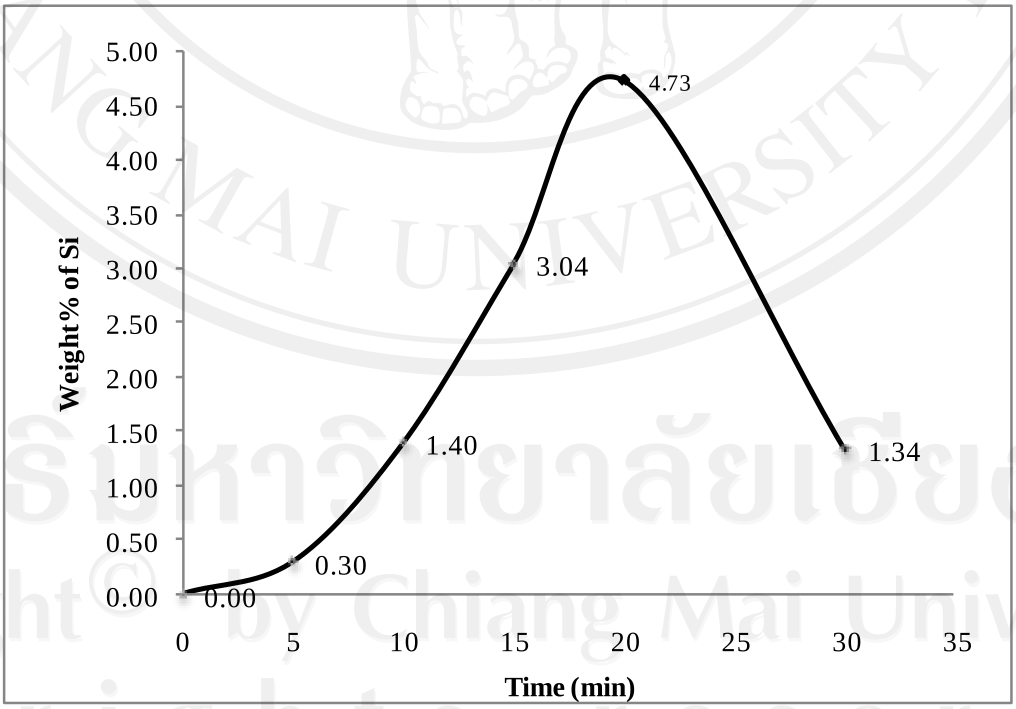

Figure 3.4 The relationship between the percentage of Si content and deposition times.

ลิขสิทธิ์มหาวิทยาลัยเชียงใหม่
Copyright© by Chiang Mai University
All rights reserved

Figure 3.4 shows the relationship between the percentage of Si and the deposition time 0-30 min. The results showed that at 20 min the amount of silica perched on the cotton surface is 4.73 percent weight of Si, and after 20 min on cotton silica is reduced. Silica reduction may be due to the agglomeration of $SiCl_4$ on the surface of cotton cloth so it became to be very large particles, and the coating is not uniform.

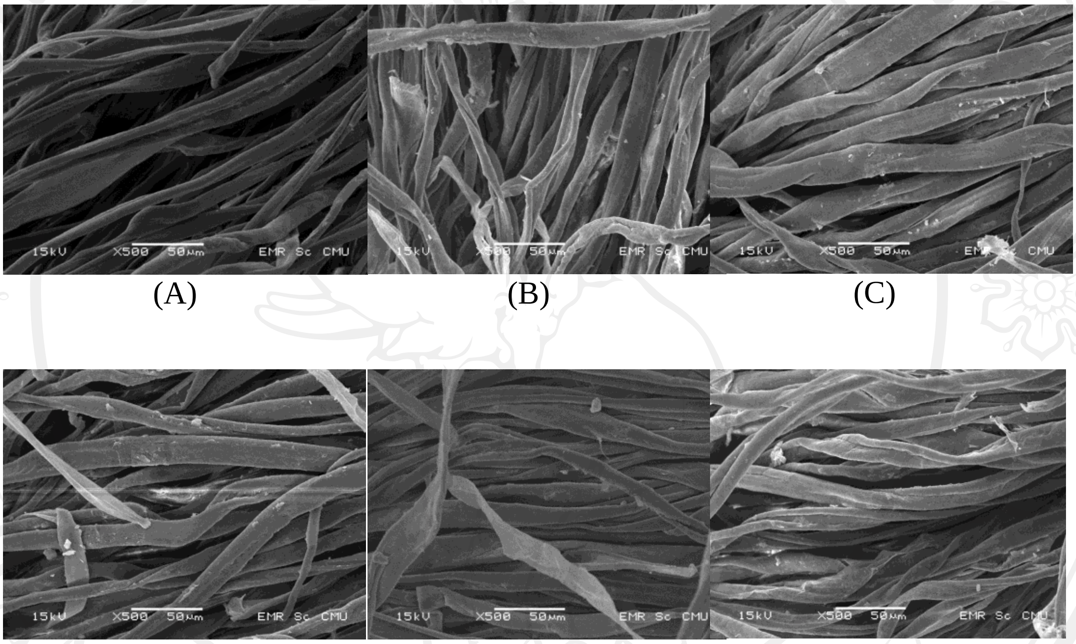

(A) (B) (C)

(D) (E) (F)

Figure 3.5 500 x magnification SEM images of the $SiCl_4$-treated cotton cloth at various deposition times (A) = 0 min, (B) = 5 min, (C) = 10 min, (D) = 15 min, (E) = 20 min, and (F) = 30 min.

Therefore, the optimum deposition time is 20 min for excellent $SiCl_4$ coverage, this condition is selected to fix and the cycle number of reaction for $SiCl_4$ deposition is varied in the next part.

3.1.2.2 Determination of the Cycle Number for Growing $SiCl_4$

The surface of the $SiCl_4$-cotton cloth which is modified by fixed deposition time at 20 min and varied cycle number at 2, 4, 6, 8, and 10 cycles are investigated by SEM at 3,000x and 500x magnification.

ลิขสิทธิ์มหาวิทยาลัยเชียงใหม่
Copyright© by Chiang Mai University
All rights reserved

From the results in Figure 3.6 and 3.7, it was found the particles of $SiCl_4$ are more growth with non-uniform structure when the cycle number rises indicating the accumulation of $SiCl_4$ deposition, while the surface of non-treated cotton show smoother surface. These results are similar to the trend in the increase of the amount of Si from solution studied by Pisuchpen *et al.* [31]. They were achieved by the reaction of poly(vinyl alcohol) fiber mats with multiple cycles of $SiCl_4/H_2O$ treatment, followed by silanization with (1H, 1H, 2H, 2H-perfluorooctyl) trichlorosilane. They fabricated PVA and PVA/silica mixtures into flexible and chemically modifiable nanostructured surfaces with varying degrees of hydrophobicity and water adhesion. The Si/C ratio, as analyzed by SEM-EDS, increased linearly with the number of $SiCl_4/H_2O$ treatment cycles (within the tested range of zero to five cycles), whereas the increase in the fiber diameters was not observed until the third treatment cycle.

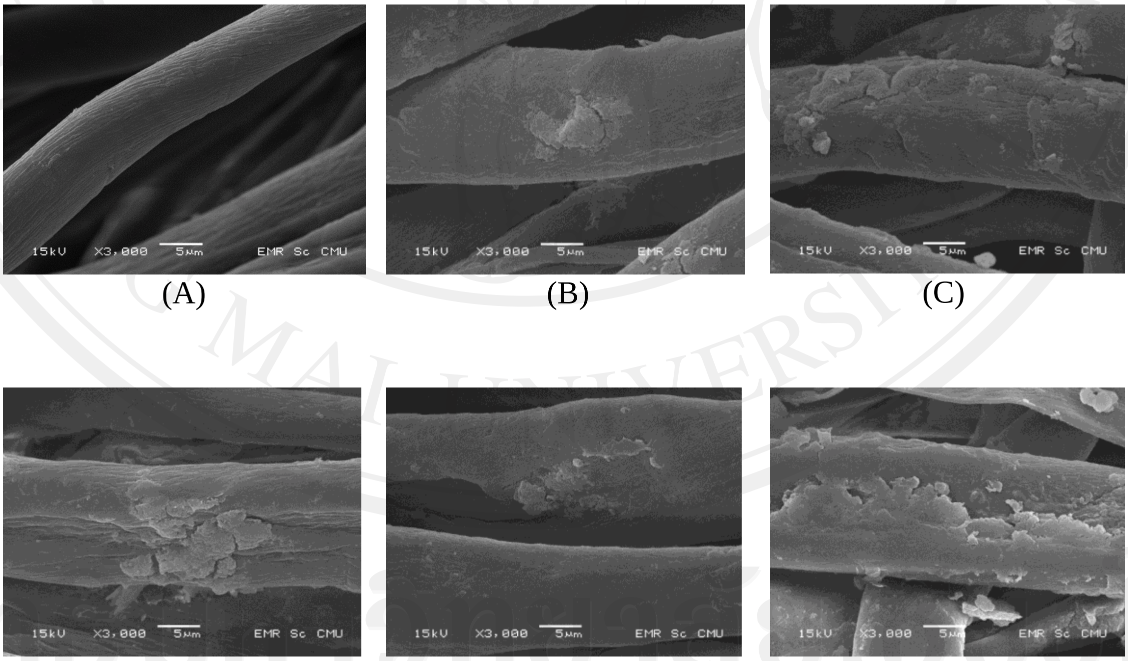

(A) (B) (C)

(D) (E) (F)

Figure 3.6 3000 x magnification SEM images of the $SiCl_4$-treated cotton cloth at various cycle number (A) = 0 cycle, (B) = 2 cycles, (C) = 4 cycles, (D) = 6 cycles, (E) = 8 cycles, and (F) = 10 cycles.

ลิขสิทธิ์มหาวิทยาลัยเชียงใหม่
Copyright© by Chiang Mai University
All rights reserved

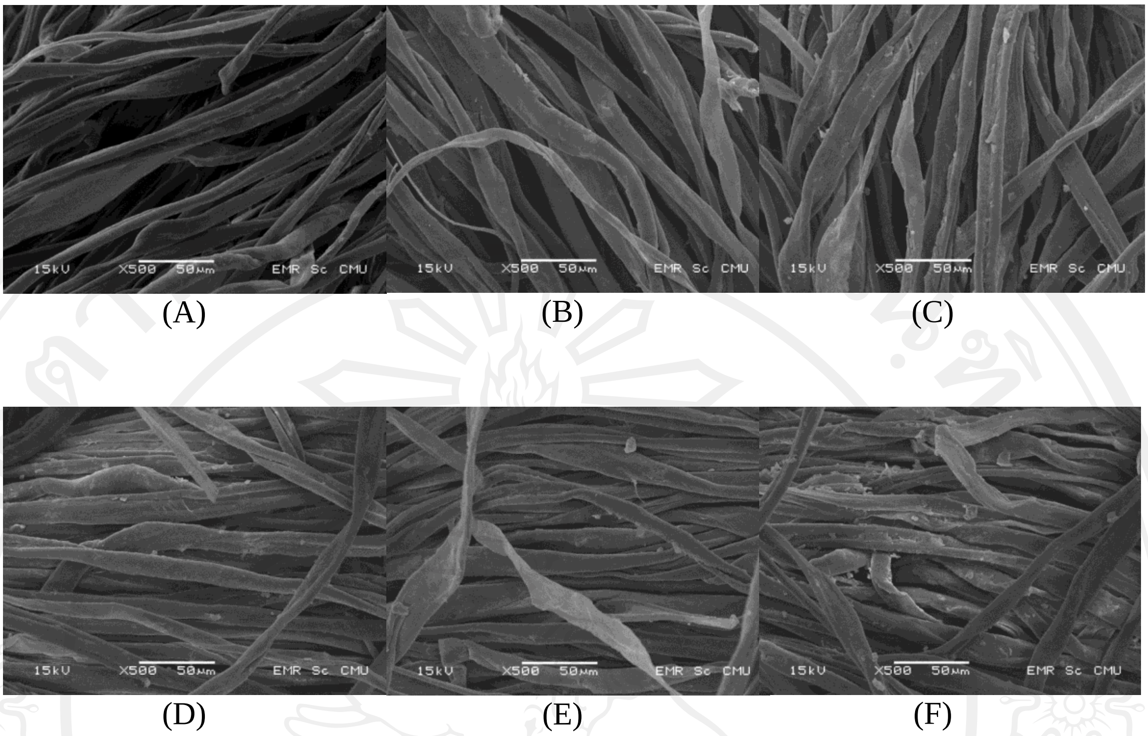

(A) (B) (C)

(D) (E) (F)

Figure 3.7 500 x magnification SEM images of the $SiCl_4$-treated cotton cloth at various cycle number (A) = 0 cycle, (B) = 2 cycles, (C) = 4 cycles, (D) = 6 cycles, (E) = 8 cycles, and (F) = 10 cycles.

In order to clearly observe the change in percentage of Si content, the EDS is employed to investigate. The relationship between percentage of Si and cycle number from 0 to 10 cycles shows that the fluctuation in Si content with the highest peak of Si content is observed at 9.13 percent weight of Si at 6 cycles, shown in Figure 3.8. The decrease and the fluctuation in Si content are observed when the cycle number above 6 cycles due to large agglomeration of $SiCl_4$ particles and non-uniform coating. Therefore, the optimum cycle number is 6 cycles due to best $SiCl_4$ coating.

ลิขสิทธิ์มหาวิทยาลัยเชียงใหม่
Copyright© by Chiang Mai University
All rights reserved

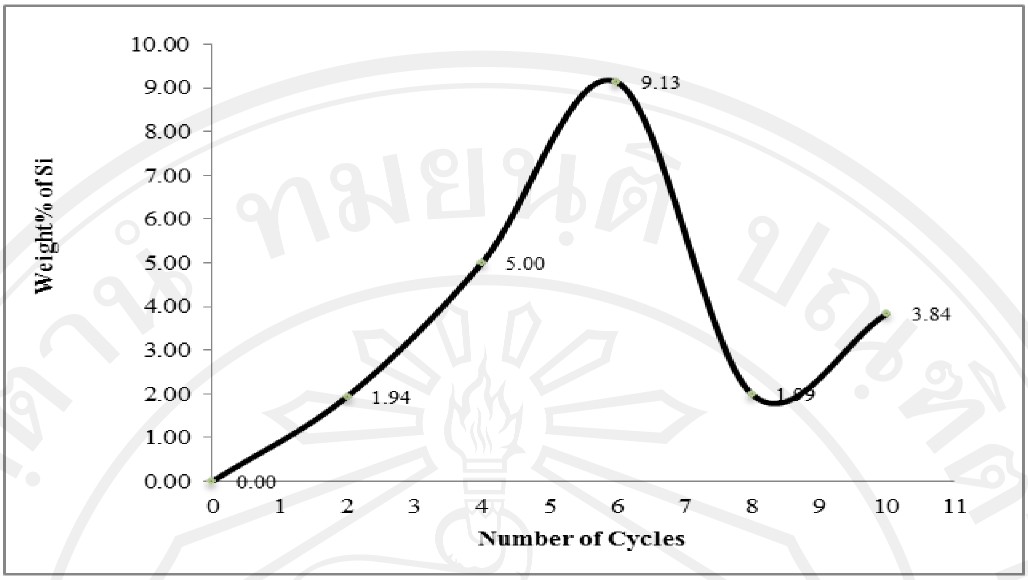

Figure 3.8 The relationship between percentage of Si content deposition on the cotton cloth versus number of cycles.

In the next part, the deposition time and the cycle number are fixed at 20 min and 6 cycles, respectively.

3.1.3 POTS-Treated Cotton Cloth, POTS-$SiCl_4$-Treated Cotton Cloth, DMDCS-Treated Cotton Cloth, DMDCS-$SiCl_4$-Treated Cotton Cloth, SA-Treated Cotton Cloth, and SA-$SiCl_4$-Treated Cotton Cloth.

Before the POTS-treated cotton cloth, POTS-$SiCl_4$-treated cotton cloth, DMDCS-treated cotton cloth, DMDCS-$SiCl_4$-treated cotton cloth, SA-treated cotton cloth, and SA-$SiCl_4$-treated cotton cloth, the $SiCl_4$-treated cotton cloth is prepared by using deposition time at 20 min for a total of 6 cycles. The deposition times for POTS is varied at 10, 30, 60, 120, and 180 min, and DMDCS is varied at 10, 20, 30, 60, and 120 min and the concentration of SA is varied from 0 M to 0.02 M. The morphology of the modified cotton cloth samples are examined by SEM and EDS.

ลิขสิทธิ์มหาวิทยาลัยเชียงใหม่
Copyright© by Chiang Mai University
All rights reserved

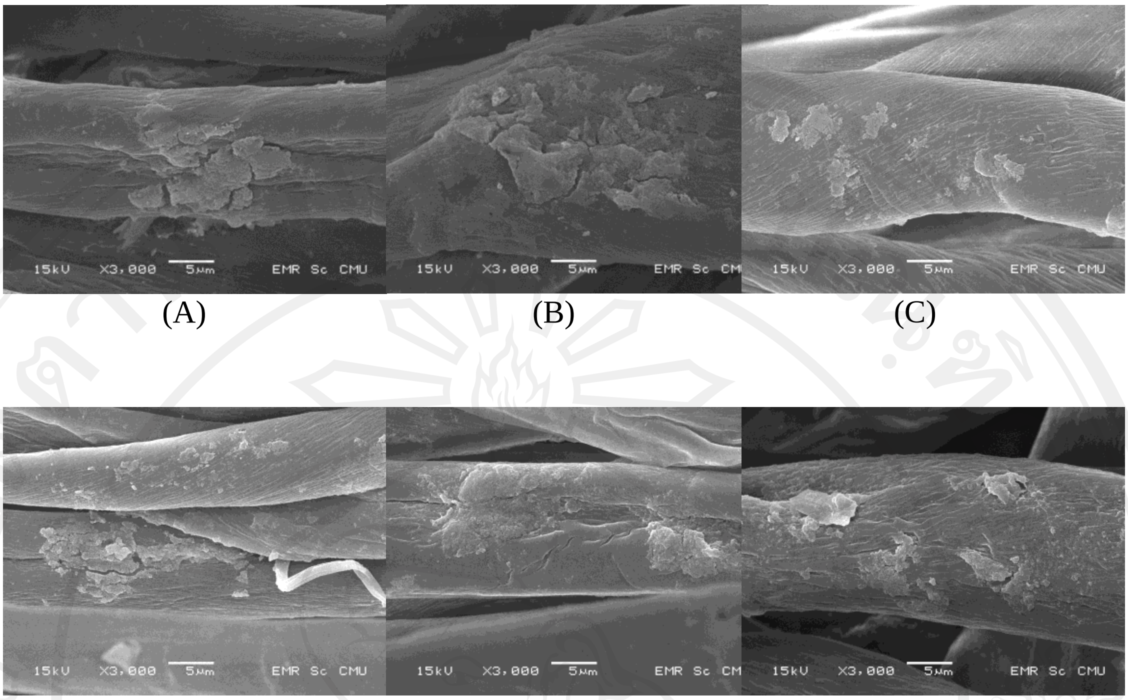

(A) (B) (C)

(D) (E) (F)

Figure 3.9 SEM images of the POTS-treated cotton cloth at various deposition times (A) = 0 min, (B) = 10 min, (C) = 30 min, (D) = 60 min, (E) = 120 min, and (F) = 180 min at 3000 x magnification.

Figure 3.9 shows that the morphology of POTS-treated cotton cloth with various deposition times is investigated by SEM at 3,000x magnification. The result shows that the particles of POTS are more growth with non-uniform structure. The modified POTS surface was rough and clustered. Figure 3.10 shows that the morphology of POTS-$SiCl_4$-treated cotton cloth with various deposition times is investigated by SEM at 3,000x magnification. The result shows that the particles of $SiCl_4$ and POTS are more growth with non-uniform structure when the cyclic number increases indicating the accumulation of $SiCl_4$ and POTS.

ลิขสิทธิ์มหาวิทยาลัยเชียงใหม่
Copyright© by Chiang Mai University
All rights reserved

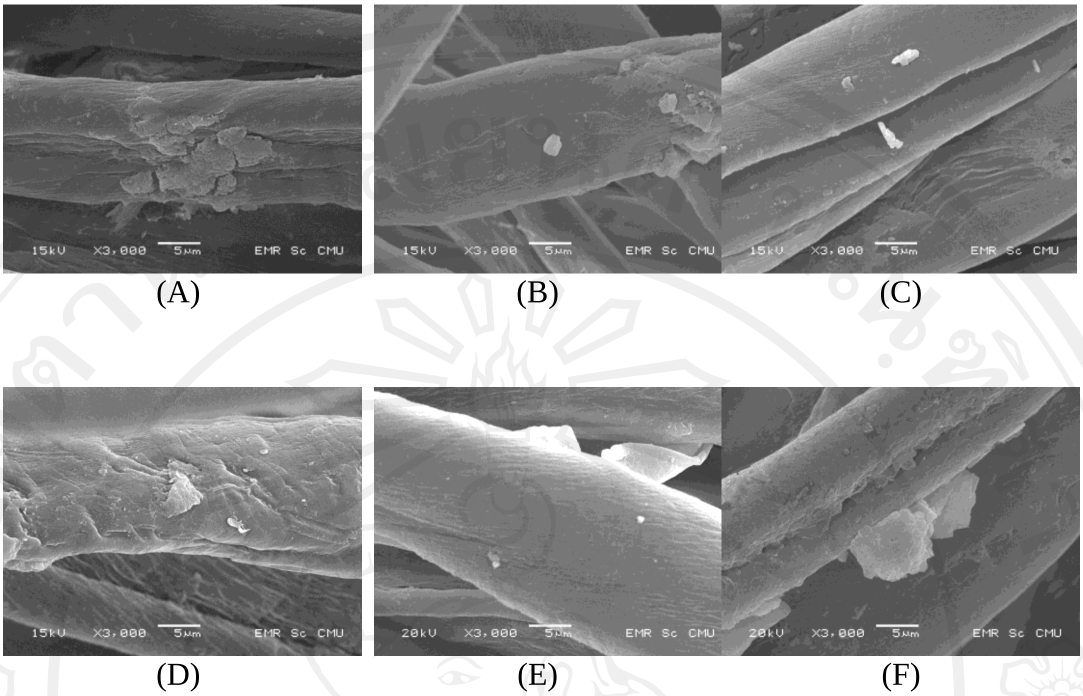

(A) (B) (C)

(D) (E) (F)

Figure 3.10 SEM images of the POTS-$SiCl_4$-treated cotton cloth at various deposition times (A) = 0 min, (B) = 10 min, (C) = 30 min, (D) = 60 min, (E) = 120 min, and (F) = 180 min at 3000 x magnification.

However, the surface of the $SiCl_4$-treated cotton cloth was not smooth. In similarly, the modified POTS surface was rough and clustered. The coatings become uniformly and densely covered by clusters of deposition various time as shown in Figure 3.10 (B)-(F). Wang *et al.* [32] fabricated superhydrophobic wood surface via a sol-gel process followed by a fluorination treatment of POTS reagent. The crystallization type of silica nanoparticles on wood surface was characterized using X-ray diffraction (XRD), the microstructure and chemical composition of superhydrophobic wood surface were described by scanning electron microscope (SEM) and energy dispersive spectrometer (EDS), the bonding force between silica nanoparticles and POTS reagent was analyzed by Fourier transform infrared spectroscopy (FTIR) and the superhydrophobic property of the treated sample was measured by contact angle (CA) measurements. The forming processes of superhydrophobic wood surface can be described as shown in Figure 3.11, which including the deposition of silica nanoparticles on the wood surface and the surface

ลิขสิทธิ์มหาวิทยาลัยเชียงใหม่
Copyright© by Chiang Mai University
All rights reserved

modification by POTS reagent. The forming processes of superhydrophobic cotton cloth surface were carried out in the same procedure.

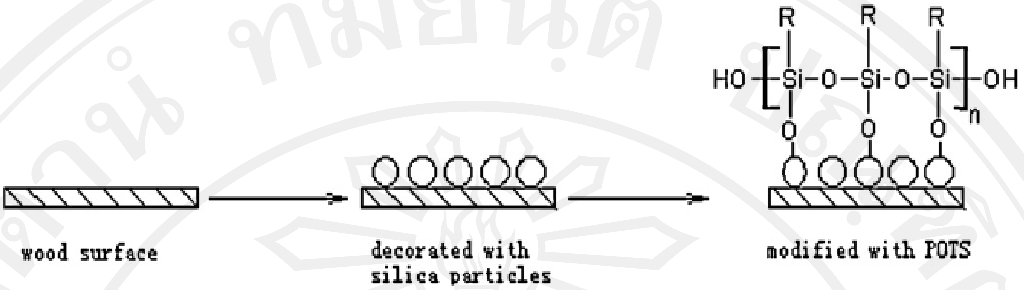

Figure 3.11 The forming processes of superhydrophobic wood surface. R represents the hydrophobic group: $-CH_2CH_2(CF_2)_5CF_3$ [32].

An analytical characterization revealed that nanoscale silica spheres stacked uniformly over the wood surface, and with the combination of the high surface roughness of silica nanoparticles and the low surface free energy film of POTS on wood surface, the wood surface has turned its wetting property from hydrophilic into superhydrophobic with a water contact angle of 164º and sliding angle less than 3º.

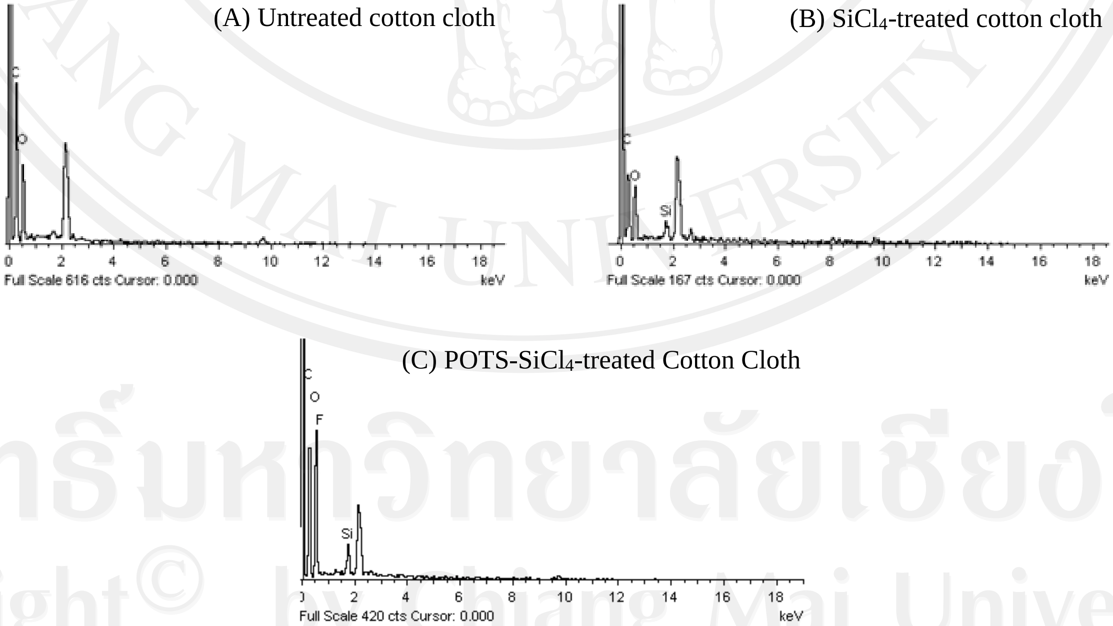
(A) Untreated cotton cloth

(B) $SiCl_4$-treated cotton cloth

(C) POTS-$SiCl_4$-treated Cotton Cloth

Figure 3.12 EDS spectra of (A) Untreated cotton cloth, (B) $SiCl_4$-treated cotton cloth, and (C) POTS-$SiCl_4$-treated cotton cloth.

ลิขสิทธิ์มหาวิทยาลัยเชียงใหม่
Copyright© by Chiang Mai University
All rights reserved

Electron dispersive X-ray spectrometer (EDS) was employed here to examine the crucial information regarding the chemical composition of hydrophobic cotton cloth surface. Figure 3.12 (A), (B) and (C) represents the EDS spectrum of untreated cotton cloth, cotton cloth surface covered with $SiCl_4$ coatings and the hydrophobic cotton cloth surface, respectively. Figure 3.11 (B) clearly shows that the elements such as C, O and Si are found in the EDS spectrum after $SiCl_4$ deposition on the cotton cloth surface and here a small amount of C element may derive from cotton cloth ingredients. From Figure 3.8 (C) was obtained when the silica nanoparticles deposited on cotton cloth surface followed by a fluorination treatment, elements such as C, O, F and Si are found in the EDS spectrum, here the C and F elements derive from POTS reagent. Thus, it can be confirmed that the POTS molecules have combined with the silica nonaparticles on the cotton cloth surface which contributes to low the surface energy of silica coatings.

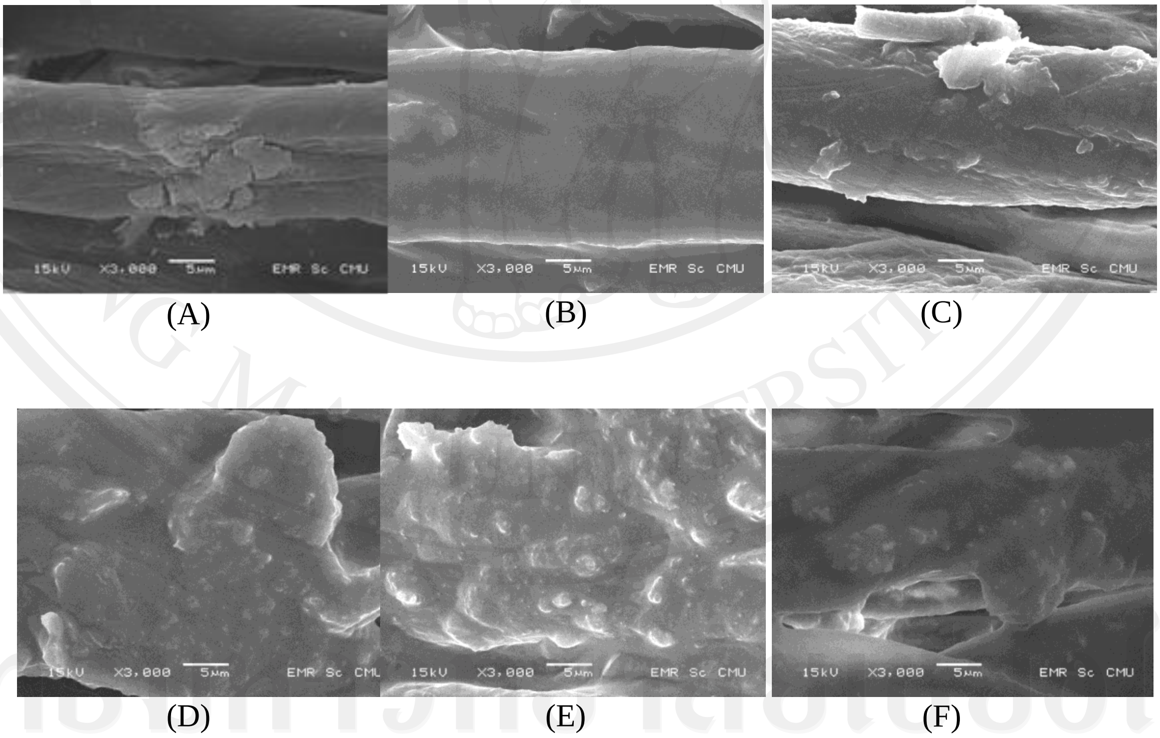

(A) (B) (C)

(D) (E) (F)

Figure 3.13 SEM images of the DMDCS-treated cotton cloth at various deposition times (A) = 0 min, (B) = 10 min, (C) = 30 min, (D) = 60 min, (E) = 120 min, and (F) = 180 min at 3000 x magnification.

ลิขสิทธิ์มหาวิทยาลัยเชียงใหม่
Copyright© by Chiang Mai University
All rights reserved

According to SEM micrographs in Figure 3.13, the transition from smooth fibers to rough after the DMDCS deposition times of 10-180 mins was achieved. Prior to silanization, silica-like (SiO_2/SiOH) inorganic layer was formed on the surface of cotton cloth. The morphology of the DMDCS- treated cotton cloth and DMDCS-$SiCl_4$-treated cotton cloth show more different compared to the POTS-treated cotton cloth and POTS-$SiCl_4$-treated cotton cloth. When the deposition time increases, the surface of the DMDCS-treated cotton cloth is more roughness with melted hydrophobic agent film of DMDCS coating, DMDCS-$SiCl_4$-treated cotton cloth shown in Figure 3.14. The DMDCS can be covered on the cotton cloth surface than that of POTS and the thickness of DMDCS film looks thicker than that of POTS. From the results of other studies, Wang *et al.* [33] studied modification of nano-fibriform silica by dimethyldichlorosilane by transmission electron microscopy, X-ray powder diffraction, infrared spectroscopy, raman spectroscopy, physical N_2 adsorption techniques, differential thermal and thermogravimetric analysis, scanning electron microscopy, and elemental analyzer. The results show that dimethylsilane derivatives have been successfully covalently grafted on nano- fibriform silica. The polarity of the modified product decreases with the substitution of -H groups by siloxyl groups. Therefore, the modified product can be easily dispersed in organic solvent and its compatibility with organic molecules is improved. After modification the pore volume decreases and the ductility greatly increases, indicating that the modified product is of a higher strength than before modification. The study demonstrates that the modified product can be used as an ideal additive to reinforce the strength of organic materials. PVA fiber mats can the reactions with dimethyldichlorosilane and methyltrichlorosilane increase the hydrophobicity of the PVA fiber mats, but they also introduce additional roughness in the form of spherical particles to the individual fibers [16]. These nanosized particles are expected to be formed as a result of crosslinked silicon-based polymeric layers via vertical polymerization of both dimethyldichlorosilane and methyltrichlorosilane.

ลิขสิทธิ์มหาวิทยาลัยเชียงใหม่
Copyright© by Chiang Mai University
All rights reserved

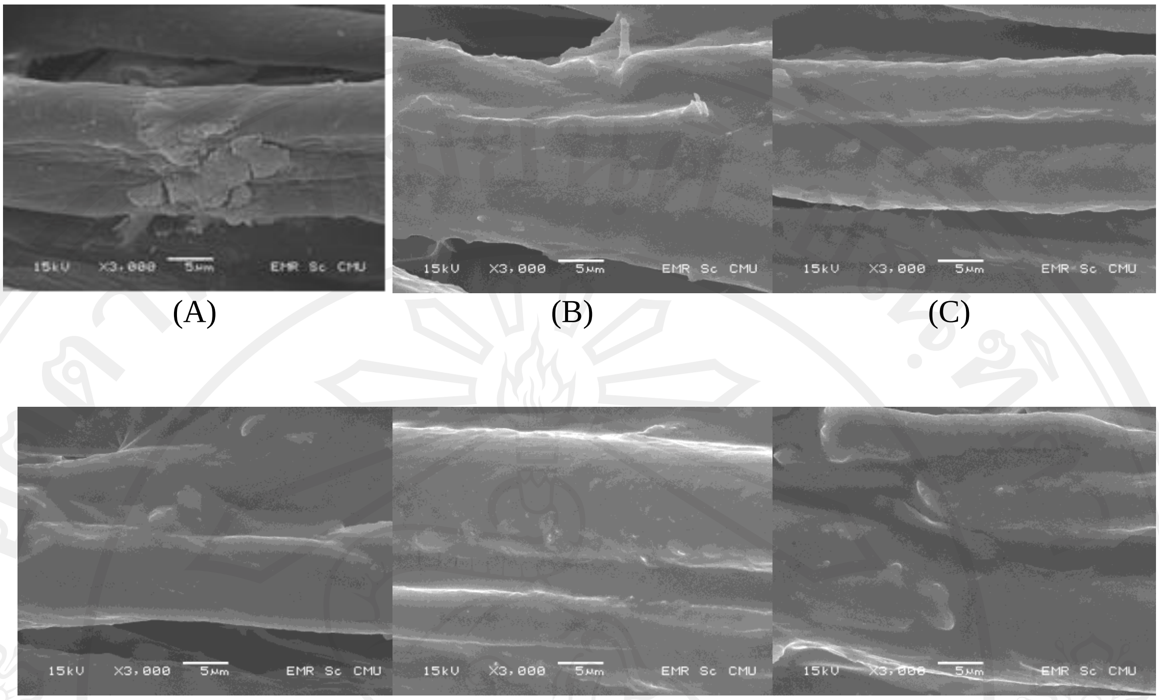

(A) (B) (C)

(D) (E) (F)

Figure 3.14 SEM images of the DMDCS-SiCl$_4$-treated cotton cloth at various deposition times (A) = 0 min, (B) = 10 min, (C) = 30 min, (D) = 60 min, (E) = 120 min, and (F) = 180 min at 3000 x magnification.

SEM-EDS enable this kind of analysis. In the case of cotton cloth samples, it was different from untreated cotton cloth and POTS-cotton cloth surface. We generally observed cotton cloth surfaces homogenously covered by elements and molecules. It is assumed that elements of exogenous origin area observed such as C, O and Si. The EDS spectra of DMDCS-SiCl$_4$-treated cotton cloth is displayed in Figure 3.15 that shows four peaks of C, O, Si and Cl indicating DMDCS coating on cotton cloth surface, here the Si and Cl elements derive from DMDCS reagent.

ลิขสิทธิ์มหาวิทยาลัยเชียงใหม่
Copyright© by Chiang Mai University
All rights reserved

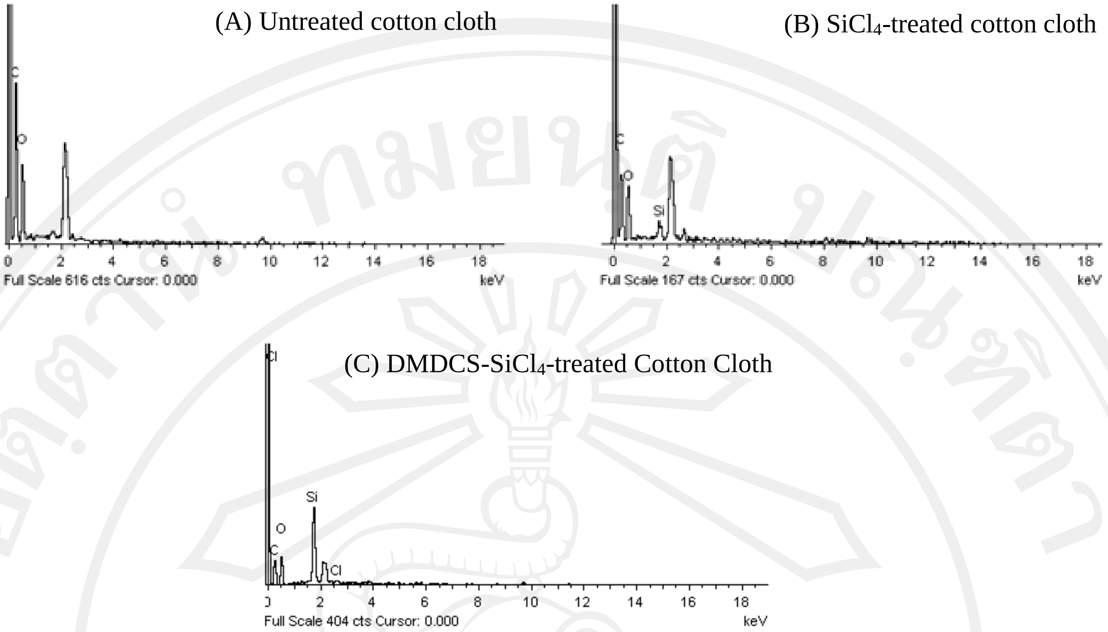

Figure 3.15 EDS spectra of (A) Untreated cotton cloth, (B) $SiCl_4$-treated cotton cloth, and (C) DMDCS-$SiCl_4$-treated cotton cloth.

Many researchers have studied the hydrophobic SA. Gurav *et al.* [34] prepared static and dynamic wettability of ZnO nanorod surface by a facile and inexpensive route. The wettability of the ZnO surface was controlled and tuned by post hydrophobization using different SA concentrations. An SEM image of the cross-section clearly reveals the SA layer on top and in between the ZnO nanorods. Surface modification by 10 mM SA resulted in heavy coverage of the SA layer on ZnO nanorods and the nanorods were hardly evident in the SEM images. After chemical modification with 2 mM SA, the hydrophilic ZnO surface switched to hydrophobic showing a static water contact angle of 116º. Wang *et al.* [35] fabricated the bionic films with hydrophobicity by the hierarchical ZnO microspheres modified by SA. It was found that the hydrophobicity of the thin films was very sensitive to the added amount of SA. The thin films modified with 8% stearic acid took on strong superhydrophobicity with a water contact angle (CA) almost to be 178º and weak adhersion. Wang *et al.* [36] studied via a simple wet chemical etching followed by SA modification, the presence of synergistic binary structures at micro- and nanometer scales and SA bestows superhydrophobic property on

ลิขสิทธิ์มหาวิทยาลัยเชียงใหม่
Copyright© by Chiang Mai University
All rights reserved

steel and aluminum alloy surfaces. The SEM images clearly indicate that the superhydrophobic surfaces of steel and aluminum alloy modified with SA have both micrometer scale structure and nanoscale structure. In summary, we fabricated superhydrophobic surfaces on cotton cloth, by wet chemical etching and surface coating of SA.

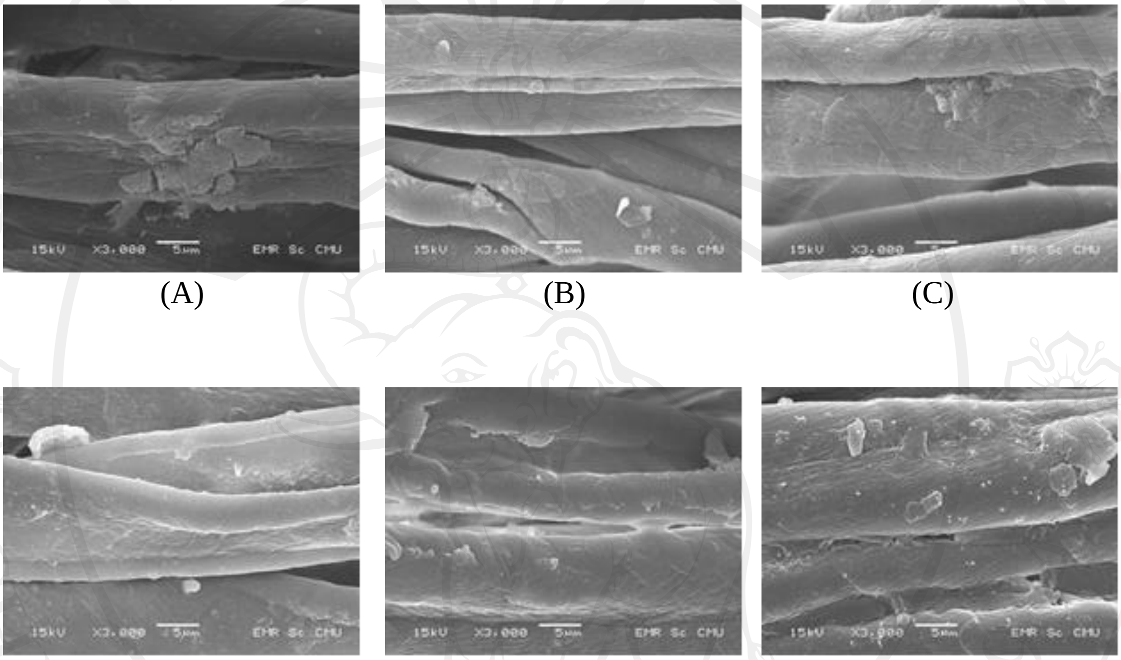

(A) (B) (C)

(D) (E) (F)

Figure 3.16 SEM images of the SA-treated cotton cloth at various deposition times (A) = 0 M, (B) = 0.005 M, (C) = 0.01 M, (D) = 0.05 M, (E) = 0.01 M, and (F) = 0.02 M at 3000 x magnification.

The morphologies of SA-treated cotton cloth and SA-$SiCl_4$-treated cotton cloth with different SA mass concentrations were shown in Figure 3.16 and 3.17. The morphology of the SA-treated cotton cloth and SA-$SiCl_4$-treated cotton cloth show more different compared to the POTS-$SiCl_4$-treated cotton cloth and DMDCS-$SiCl_4$-treated cotton cloth. When the concentration of SA increases, the surface of the SA-$SiCl_4$-treated cotton cloth is smoother more than the surface of the SA-treated cotton cloth. It could be observed that the more concentration of SA showed a smoother. The SA is more cover coating on the cotton cloth surface than that of POTS.

ลิขสิทธิ์มหาวิทยาลัยเชียงใหม่
Copyright© by Chiang Mai University
All rights reserved

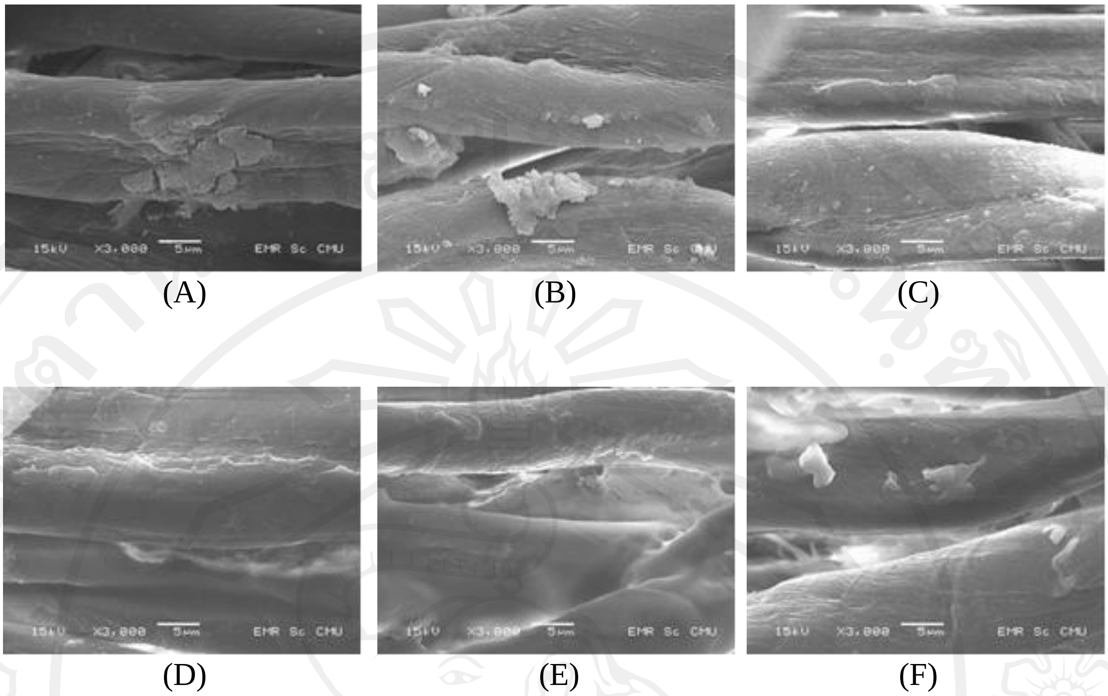

(A) (B) (C)

(D) (E) (F)

Figure 3.17 SEM images of the SA-$SiCl_4$-treated cotton cloth at various deposition times (A) = 0 M, (B) = 0.005 M, (C) = 0.01 M, (D) = 0.05 M, (E) = 0.01 M, and (F) = 0.02 M at 3000 x magnification.

3.2 Characterization of Functional Groups by Fourier Transform Infrared Spectroscopy (FTIR)

The functional groups related to the modification of $SiCl_4$ were studied by FTIR operating at room temperature in range of 4000-400 cm^{-1}, which are assigned to O-H stretching vibration and C-O stretching vibration respectively. The FTIR spectra of both the untreated cotton cloth and the $SiCl_4$-treated cotton cloth are displayed in Figure 3.18.

ลิขสิทธิ์มหาวิทยาลัยเชียงใหม่
Copyright© by Chiang Mai University
All rights reserved

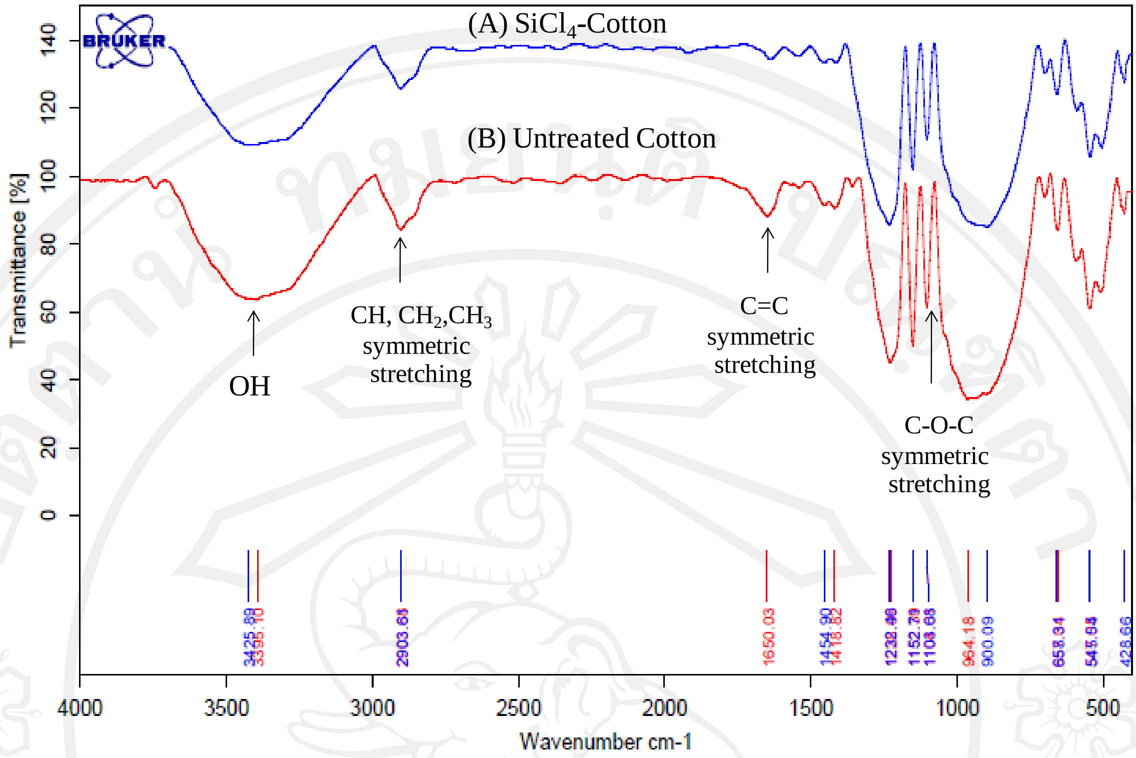

Figure 3.18 FTIR spectra of (A) $SiCl_4$-treated cotton cloth and (B) untreated cotton cloth.

The spectra show the similar spectra. The peak area variations of the O-H stretching vibration (3700-3100 cm^{-1}) against the temperature are shown. Four kinds of inter-chain hydrogen bonds and intra-chain hydrogen bonds can be identified, which are 3461 cm^{-1} (intra-chain v_1), 3478 cm^{-1} (intra-chain v_1'), 3369 cm^{-1} (intra-chain v_2) and 3409 cm^{-1} (inter-chain v_3). 3478 and 3461 cm^{-1} are possible from the same hydroxyl groups, and 3461 cm^{-1} is assigned to the intra-chain hydrogen bonded hydroxyl groups with the participating of the water molecules [37]. Thus, the broad peak at 3425 and 3395 cm^{-1} are attributed to the functional group O-H vibrations.

The small broad peak at 1638-1643 cm^{-1} is attributed to CH, CH_2, and CH_3 symmetric stretching. Moreover, the shape peaks at the 1313-1427 cm^{-1} and 1023 - 1280 cm^{-1} are attributed to the oscillation frequency of the functional group CH_3 and C-OH, respectively. However, the peaks of $SiCl_4$ do not appear because there may be a lower concentration in the ppm scale. However, the $SiCl_4$-treated cotton cloth surface exhibited more wettability than the untreated cotton cloth, a characteristic of the $SiCl_4$-

ลิขสิทธิ์มหาวิทยาลัยเชียงใหม่
Copyright© by Chiang Mai University
All rights reserved

treated cotton cloth which has been fabricated by POTS, DMDCS, and SA modification.

In general, the cotton cloth exhibits several relatively strong absorption bands. These bands are associated with the vibration in COH group, the structure unit common to these molecules. Tetsuo Kondo [38] characterized hydrogen-bonding formation in amorphous cellulose by the analysis of Fourier transform infrared (FTIR) spectra. In other words, the O-H bands in the artificial spectrum were considered to be simply a sum of hydrogen-bond absorptions contributed by each individual spectrum. The artificial spectrum was then compared to an experimental spectrum for an amorphous cellulose sample. The IR bands of amorphous cellulose were characterized as shown in Table 3.1 Absorption frequency is similar to the result of FTIR spectra of cotton cloth.

Table 3.1 Comparison of typical absorption band frequencies for the real and the artificial IR spectra of amorphous cellulose.

Frequency (cm^{-1})		**Relative intensity**	**Interpretation**
Real	**Artificial**		
669	671	W	OH out-of-plane bending
899	892	M	Antisymmertric out-of-phase ring stretching
1070	1075	S	Skeletal vibrations involving C-O stretching
1159	1154	S	Antisymmertric bridge C-O-C stretching
1374	1375	M	CH bending
1420	1425	W	CH_2 symmetric bending
2892	2903	M	CH stretching
3420	3457	S	OH stretching

S = strong; M = medium; W = weak

ลิขสิทธิ์มหาวิทยาลัยเชียงใหม่
Copyright© by Chiang Mai University
All rights reserved

3.3 X-Ray Diffraction (XRD)

X-ray diffraction (XRD) pattern is a suitable method to identify the crystalline structure of the samples. The XRD patterns shows peaks at 12º and 21º, which can be attributed to the crystalline structure of cellulose. Lu *et al.* [39] obtained morphological, crystalline, thermal and physicochemical properties of cellulose nanocrystals from sweet potato residue. XRD analysis indicated that the cellulose nanocrystals retained the cellulose I crystalline structure, with a crystallinity of approximately 72.53%. TGA curves showed that the decomposition temperature of nanocrystals was decreased. Gindl *et al.* [40] studied the structural changes during tensile testing of an all-cellulose composite by in situ synchrotron x-ray diffraction. Tensile experiments with a regenerated cellulose film reinforced by microcrystalline cellulose, combined with simultaneous synchrotron wide angle X-ray scattering, show that, when mechanically loaded at constant strain rates, the cellulose crystallites tend to orient with their crystallographic c-axis parallel to the force direction and an irreversible preferred orientation is induced. X-ray diffractograms collected from microcrystalline cellulose, pure regenerated cellulose, and from a regenerated cellulose film reinforced by Aldrich microcrystalline cellulose show the different crystalline structure of these materials (Figure 3.19).

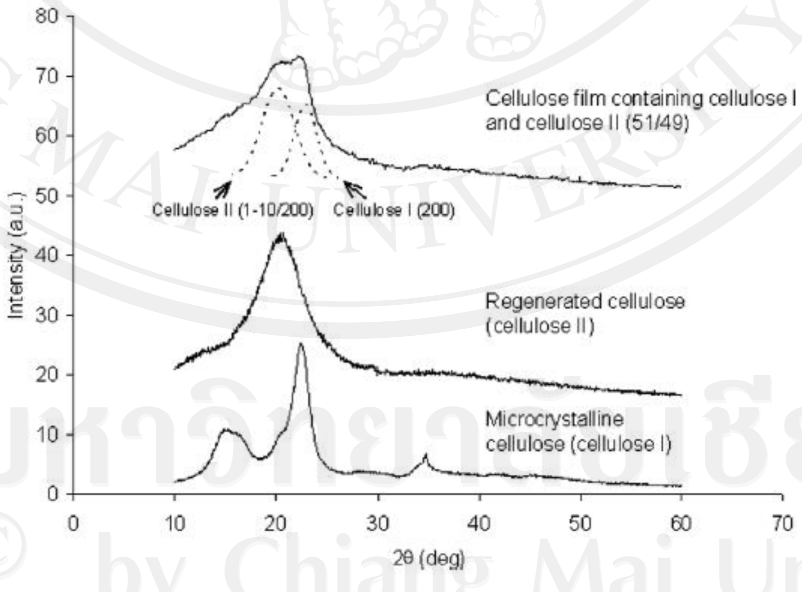

Figure 3.19 X-ray diffractograms of microcrystalline cellulose, regenerated cellulose, and an all cellulose composite film containing cellulose I and cellulose II [40].

ลิขสิทธิ์มหาวิทยาลัยเชียงใหม่
Copyright© by Chiang Mai University
All rights reserved

Shuliang Wang [33] was characterized crystallization type of silica nanoparticles on wood surface by X-ray diffraction (XRD). The surface modification of silica nanoparticles on wood surface was carried out by the chemical vapor deposition of POTS reagent. Briefly, the silica-coated wood sample was placed into a sealed vessel containing about 0.3 ml of POTS reagent. Figure 3.20 represents the XRD patterns of the pristine poplar wood and the superhydrophobic coatings, respectively. There are two strong diffraction peaks at about 2θ = 15.8º and 22º, as shown in Figure 3.20 (A). Also, there was a strong diffraction peak at about 2θ = 23º in Figure 3.20 (B), the diffraction peak can be indexed to silica crystal (JCPDS No. 2920085) and no other phases were detected.

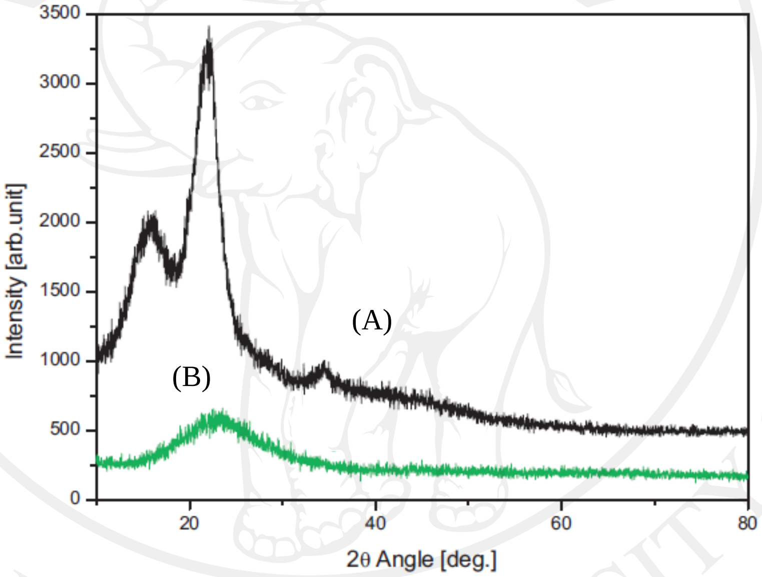

Figure 3.20 X-ray diffraction patterns of (A) pristine poplar wood and (B) superhydrophobicity coatings [33].

XRD is employed to investigate crystalline of POTS-treated cotton cloth, DMDCS-treated cotton cloth, SA-treated cotton cloth, POTS-$SiCl_4$-treated cotton cloth, DMDCS-$SiCl_4$-treated cotton cloth, and SA-$SiCl_4$-treated cotton cloth, shown in Figure 3.21. All data is described by following;

ลิขสิทธิ์มหาวิทยาลัยเชียงใหม่
Copyright© by Chiang Mai University
All rights reserved

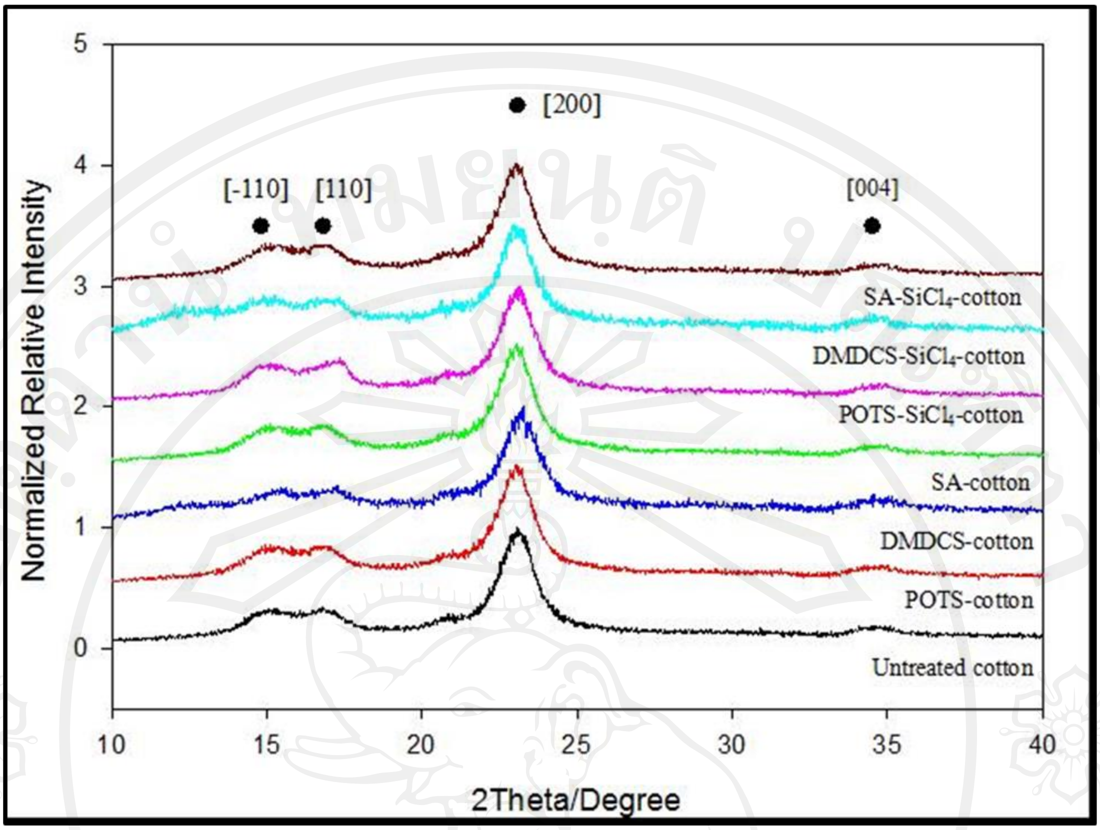

Figure 3.21 XRD patterns of cotton cloth; untreated cotton cloth, POTS-treated cotton cloth, DMDCS-treated cotton cloth, SA-treated cotton cloth, POTS-$SiCl_4$-treated cotton cloth, DMDCS-$SiCl_4$-treated cotton cloth, and SA-$SiCl_4$-treated cotton cloth.

The XRD patterns for all samples show the typical four peaks of cellulosic material of [-110], [110], [200], and [004] at 2θ equal to 14.8º, 16.3º, 22.6º, and 34.3º, respectively. No other peaks were observed in the diffractograms of the treated samples. That indicated the same crystalline structures of the cotton cloth before and after coating with POTS, DMDCS, SA, POTS-$SiCl_4$, DMDCS-$SiCl_4$ and SA-$SiCl_4$ due to the physical adsorption and concentration of the coating adhered to the surface is minimal. Therefore, the cotton cloths with all addition species were formed as composites.

ลิขสิทธิ์มหาวิทยาลัยเชียงใหม่
Copyright© by Chiang Mai University
All rights reserved

3.4 Water Contact Angle (WCA)

The presence of hysteresis becomes critical with regards to superhydrophobic surfaces (as defined by a static or advancing WCA > 150º). Superhydrophobic surfaces are often correlated with water repellency, but the presence of hysteresis on a superhydrophobic surface might disguise such behavior as it causes water drops to stick to the surface. Water droplets easily roll off superhydrophobic surfaces if the WCA hysteresis is below ~10º, depending on the size of the drops. For larger WCA hysteresis, water droplets tend to stick even to superhydrophobic substrates with advancing CA greater than ~150º. As a result, the functional classification of superhydrophobic substrates depends on CA hysteresis. For study contact angle measurements, a 1 μL deionized water drop and analyzed by using image analysis software were used. To investigate hydrophobicity or wettability of untreated cotton cloth, POTS-treated cotton cloth, DMDCS-treated cotton cloth, SA-treated cotton cloth, POTS-$SiCl_4$-treated cotton cloth, DMDCS-$SiCl_4$-treated cotton cloth, and SA-$SiCl_4$-treated cotton cloth, contact angle of water droplet on the sample surface is measured. If the contact angle of water droplet is less than 90º, the surface is classified as hydrophilic. Otherwise, if the contact angle of water droplet is greater than 90º, then it is classified as hydrophobic.

Figure 3.22 shows the degree of the water droplet on the sample cotton cloths. The degrees of water droplet on POTS-treated cotton cloth and DMDCS-treated cotton cloth are 132º and 120º, respectively, indicating POTS exhibits the more hydrophobicity than that of DMDCS. Furthermore, when the $SiCl_4$ is coated on the first layer, the degree of water droplet increases to reach 155º and 138º for POTS-$SiCl_4$-treated cotton cloth and DMDCS-$SiCl_4$-treated cotton cloth, respectively. Thus, the thin film of $SiCl_4$ as the first layer improves hydrophobic property. In the other hand, the degree of water droplet on SA-treated cotton cloth and SA-$SiCl_4$-treated cotton cloth shows about 142º. Thus, the order of hydrophobicity for all samples is Untreated cotton < DMDCS-treated cotton cloth < POTS-treated cotton cloth < DMDCS-$SiCl_4$-treated cotton cloth < SA-$SiCl_4$-treated cotton cloth < SA-treated cotton cloth < POTS-$SiCl_4$-treated cotton cloth, while that with $SiCl_4$ is DMDCS-$SiCl_4$ < SA-$SiCl_4$ < POTS-$SiCl_4$. All degree of water droplet on the different samples is summarized in Table 3.2.

ลิขสิทธิ์มหาวิทยาลัยเชียงใหม่
Copyright© by Chiang Mai University
All rights reserved

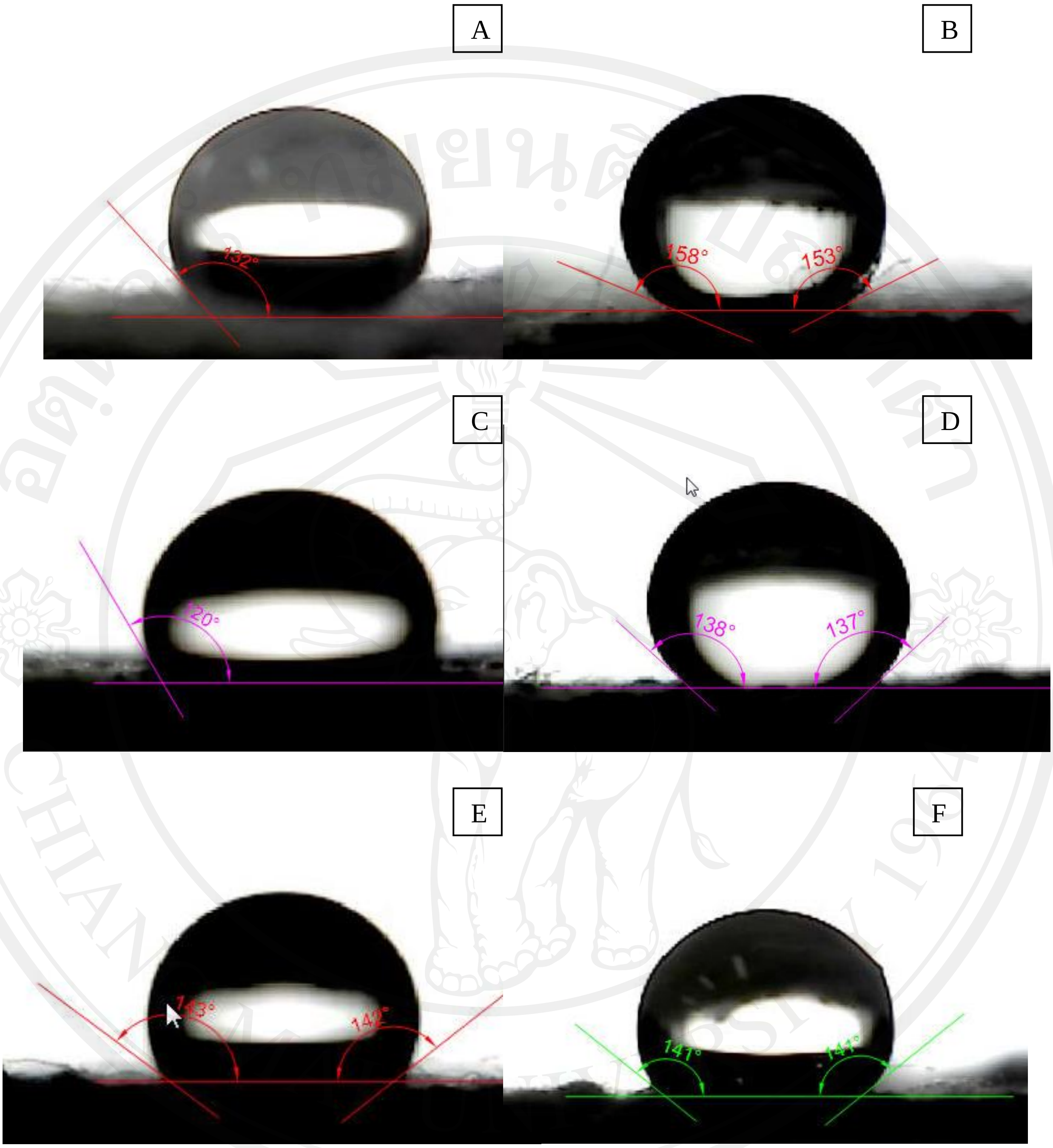

Figure 3.22 Water contact angle of (A) POTS-treated cotton cloth, (B) POTS-$SiCl_4$-treated cotton cloth, (C) DMDCS-treated cotton cloth, (D) DMDCS-$SiCl_4$-treated cotton cloth, (E) SA-treated cotton cloth, and (F) SA-$SiCl_4$-treated cotton cloth.

ลิขสิทธิ์มหาวิทยาลัยเชียงใหม่
Copyright© by Chiang Mai University
All rights reserved

Table 3.2 Water contact angles (WCA) of untreated cotton, POTS-treated cotton cloth, POTS-$SiCl_4$-treated cotton cloth, DMDCS-treated cotton cloth, DMDCS-$SiCl_4$-treated cotton cloth, SA-treated cotton cloth, and SA-$SiCl_4$-treated cotton cloth.

Sample	**Water contact angle (º)**
Untreated cotton cloth	69
POTS-treated cotton cloth	132
POTS-$SiCl_4$-treated cotton cloth	158
DMDCS-treated cotton cloth	120
DMDCS-$SiCl_4$-treated cotton cloth	138
SA-treated cotton cloth	142
SA-$SiCl_4$-treated cotton cloth	141

The fact that the advancing and receding contact angle are similar for two type of the SA-treated cotton cloth and SA-$SiCl_4$-treated cotton cloth shows that differences in micro- and nano-scale surface roughness due to variations in modified $SiCl_4$ do not much significantly affect the “sticky” superhydrophobic behavior.

ลิขสิทธิ์มหาวิทยาลัยเชียงใหม่
Copyright© by Chiang Mai University
All rights reserved